Dynamic Characteristics of Repetitive Shock Machines

By
George R. Henderson
GHI Systems, Inc.

A review of methods for measuring the ability of vibration to cause product defect precipitation through fatigue accumulation. Emphasis is given to estimating fatigue accumulation during tests, either at shaker table surfaces, or on products. The methods described may be used to estimate fatigue accumulation rates for both Gaussian and non-Gaussian vibration, making them useful for all types of shakers, as well as for real field environments. Examples are given for highly accelerated life tests (HALT). Additional measurements techniques used to determine machine and product resonances, spectrum modification, and transmissibility are also described. Examples are given for a product undergoing stress screening.

This technical paper will be presented at the
IES National ATM in Las Vegas
During May 1993.

It is also being published in the
Proceedings of The Instituite of Environmental Sciences
May 1993.

DYNAMIC CHARACTERISTICS OF REPETITIVE SHOCK MACHINES

George R. Henderson
GHI Systems, Incorporated

George Henderson is President of GHI Systems, Inc., which he founded in 1978. Prior to that time, Mr. Henderson was a Principal Scientist at E. H. Plesset Associates Division of EG&G, Inc., where he was in charge of large scale atmospheric data acquisition experiments employing lasers. In addition, Mr. Henderson has consulted for various clients in the field of data acquisition and analysis. Mr. Henderson is a graduate of Utah State University with a degree in Electronics Engineering, and is a Senior Member of IES, and ASTM.

ABSTRACT.

The non-Gaussian characteristics of repetitive shock machines, used for commercial product stress testing are discussed. Problems relating to the use of ASD and RMS methods for estimating fatigue accumulation for non Gaussian loads are described. A peak probability distribution function for evaluating non-Gaussian vibration is described. An accumulated fatigue damage factor for estimating relative screen intensity, using the peak probability distribution function is developed. Illustrations of all analysis techniques are presented for both electrodynamic and repetitive shock machines.

KEY WORDS. Vibration, stress, fatigue, Miner's Rule, autospectral density (ASD), root mean square (RMS), peak probability distribution function (PPDF), accumulated fatigue damage factor (AFDF).

I. INTRODUCTION

Over the last dozen years, a new branch of product screen testing has evolved which differs markedly from its ESS genesis. This branch has as its objective the rapid precipitation of latent product design and production faults. The singular characteristic of CSS that sets it apart from traditional ESS is the use of higher stress levels in order to achieve defect detection in the shortest time possible. The technology is presently practiced more by commercial rather then defense and aerospace firms, although the techniques would seem to apply to both. Lacking a more formally bestowed name, it seems appropriate to refer to commercial stress screening as CSS.

It is possible to achieve a degree of success in CSS using traditional shakers, such as electro dynamic (ED) and servo hydraulic (SH), given longer allowable test durations. A new class of machine is fast finding acceptance for CSS. This machine is based on the use of repetitive shocks to induce high levels of response, and hence fatigue accumulation in items under test. Again, for lack of a formal name, these machines are referred to as repetitive shock, or RS machines, in this paper. These machines employ air driven impact hammers attached to modal tables onto which products are fixtured. The fundamental reason for RS machine acceptance is their ability to reduce defect detection and precipitation time.

With the adoption of RS machines, changes in the vibration measurement paradigm are necessary. ED machines produce Gaussian excitations with amplitude probability distributions (PDF's) limited to 3σ ranges. Because we know the distribution range and shape of Gaussian vibration, we use root mean square, RMS and autospectral density, ASD, methods to characterize machines producing this type of excitation. In addition, we can indirectly estimate the key parameter of interest, fatigue accumulation, because we know the relationship between 3σ Gaussian vibration and stress. Even though this is true, the estimation of fatigue by RMS and ASD tools is tedious, i.e., neither method yields a direct measurement of peak amplitudes or loading rates.

In the case of RS machines, excitations are not Gaussian and hence the assumptions we make when using RMS and ASD when analyzing their fatiguing ability are no longer valid. What is needed are measurement techniques that give a direct estimate of stress producing abilities for non-Gaussian excitations.

Since accumulated fatigue is the product of the number of applications of stress and its magnitude, then it follows that techniques relating to measurement of peaks and loading rates are appropriate.

The purpose of this paper is to describe methods for estimating relative fatigue-producing intensity of both Gaussian and non-Gaussian excitations. These methods may be applied to all types of vibration machines. However, their most significant application is the characterization of the non-Gaussian vibration produced by RS machines.

This paper describes techniques based on the measurement of acceleration peaks and loading rates. These techniques are known as peak probability density function, PPDF, and accumulated fatigue damage factor, AFDF. Both techniques were derived from related technologies used in the measurement of vibration induced fatigue. Illustrations of their application are presented including their use to characterize both ED and RS machines.

An exhaustive review of stress event loading analysis techniques for the purpose of fatigue assessment for vehicles has been produced by Ashmore, Piersol, and Witte [1].

At the time the original version of this paper was being prepared for the October 1992 IES ESSEH meeting in Baltimore, a paper for the same meeting was being written by Ed Szymkowiak [2]. While the Szymkowiak paper was written more from the point of view of the relationship of ESS vibration testing to service life, it is significantly parallel in its approach and conclusions to this paper. It is strongly suggested that the Szymkowiak paper be read by those interested in CSS and RS machine technology.

II. BACKGROUND OF RS MACHINES

The RS machine as a commercial product is a relatively new concept in fatigue testing, although impact hammer exciters like those used in the typical RS machine have been employed for years in the military and aerospace area for such tasks as simulating repetitive gunfire. Firms which produce RS machines attach similar hammers to tables of various designs and enclose the combination in thermal chambers. The result is a machine intended to provide both thermal and vibration stress to a product.

An earlier paper [3] describes the mechanics of RS machines. At the risk of being repetitious with the earlier paper, it is important to list the characteristic features of these machines to better understand the analysis techniques that follow.

- The RS machine is capable of producing broadband excitations of up to hundreds of gRMS,
- The RS machine produces excitations in three orthogonal directions (triaxial) simultaneously, thus reducing the need for product reorientation to test all axis.
- The RS machine produces rotational accelerations about the principal axes,
- RS machine excitation has a very broad range of amplitude (σ magnitude), with some RS machines measured at greater than 10σ, and
- RS machine stress loading per unit time is very high.

The oscillation rate of a single hammer is typically 30Hz to 50Hz. Each shock produces a damped sine wavelet. Multiple hammers are attached to a modal table at various orientations. Over a time period of seconds, the effect of table modes and techniques of hammer frequency and amplitude modulation, contribute to the overall spectral continuum of the RS machine. This results in a complex, broadband excitation from the low tens of Hz up to several thousand Hz which is roughly stationary and random-like.

Measurements at the table surface on an RS machine indicate high excitation levels in the three basic x, y, and z triaxial dimensions of the table. In addition, transmissibility and coherence measurements have shown that at any instant of time, acceleration vectors at different locations can have high magnitudes of acceleration and no phase correlation, giving proof that RS machines produce rotation couples about the three major axis of the system. However, it must be pointed out that the magnitudes of velocity and displacement of an RS machine table, particularly at low frequency and in the plane of the table are very small.

The spectrum of the RS machine is fixed by design but can change with loading and fixturing due to impedance mismatching. This relates to the fact that any high modal density of the table may be greatly changed by improper mounting point impedance matching. This allows the product to interact with the table. For a discussion of multi-mode fixtures, and problems due to mounting point impedance, see Scharton [4], [5].

III. SHAKER ANALYSIS METHODS

To understand which measurement techniques apply to RS machines, a quick overview of analysis methods is in order. Some of these techniques apply to Gaussian and some to non-Gaussian data. These techniques are:

- Spectral Power Density, ASD,
- Root Mean Square, RMS,
- Shock Response Spectrum, SRS.
- Acceleration Peak Probability Distribution Function, PPDF, and

- Accumulated Fatigue Damage Factor, AFDF.

ASD

The ASD method is the most widely used to measure vibration. Briefly, ASD analysis results in a plot of average acceleration power per cycle of analysis bandwidth. Any information on the magnitude of transient acceleration peaks is lost when the component FFT records are averaged. Hence, the result is an incomplete measure of the most stressful portion of an excitation.

While the ASD provides a valid average spectral description for all stationary random signals, independent of their statistical probability distributions, PDF, the ASD gives no information about the peak amplitude domain, nor the loading rate properties of a signal.

The ASD is used mainly for excitations that have a normal Gaussian PDF. This type of excitation is characterized as being 3σ limited, i.e., having no peaks exceeding three times the standard deviation. The Gaussian assumption for ASD analysis works in the favor of ED machines where normal Gaussian excitation is the norm.

RS machine excitation, as well as many field environments, exceed 3σ PDF's. It follows that analysis methods which are optimum for Gaussian PDF's may not accurately characterize excitations with non-Gaussian PDF's. This is exactly the case with the RS machine as well as many field environments.

RMS

RMS is another widely used analysis tool. It gives a valid measure of average intensity of all signals, independent of their PDF's. However, like the ASD, it is more descriptive of Gaussian signals because we assume additional information about that type of data. As such, RMS has the same problems for non-Gaussian vibration as ASD.

It can be easily shown that two very dissimilar excitations can have the same ASD, but will have very different stress producing potentials. For example, a constant amplitude sine wave will have an RMS value of 0.707 of peak, while an environmental signal, having the identical RMS, can have peaks that are 10's or 100's times higher than the peaks of the former. Example: Potholes with high stress transients in an otherwise low stress smooth highway vibration record.

Even though they occur less often than 1σ excitation peaks, the importance of high stress peaks is that fatigue is a product of their amplitudes. When stress levels are low, some materials will not fail even at extremely high loading totals. On the other hand, some materials will fail with a very few loadings of very high σ levels. The relation between the number of loadings and the magnitude of stress for fatigue failure is known as the S-N curve. The negative slope of this curve, knows as "b" ranges between 6 and 25 for various materials. Copper without stress intensification is 10, with defects, as low as 6.5. This power function is utilized in Miner's Rule, which is discussed later.

SRS

SRS analysis was developed originally for use with ongoing vibration containing transient peaks. Its present principal use for transient shock analysis has led to much confusion as to its validity for use with vibration. It was first proposed in the 30's for use with structural analysis of buildings subjected to seismic (earthquake) vibration [6]. Since that time, SRS has been adopted by Bell Labs as well as the IEEE as a vibration analysis tool for seismic vibration testing of communications equipment. In reality, SRS is a time domain function sensitive to the peaks of an excitation. A recent paper by Smithson suggested SRS use in ESS testing [7].

One problem with SRS is that different excitations with drastically different time durations can produce the same SRS. Because of this problem, fatigue accumulation may not be accurately estimated with its use. However, if two segments of equal time from an ongoing dynamic or stationary random function are analyzed, they will produce essentially the same SRS. Over periods of seconds, excitation from RS machines is ongoing dynamic. In this case, when used correctly, SRS is a valuable analysis tool describing peak amplitudes versus frequency, assuming certain factors about component response.

SRS can be used to qualify an excitation. MIL-STD-810C, D and E as well other product related specificat-ions favor SRS as the preferred method of specifying environmental excitation for laboratory simulation. These specifications range from product response to transient shock down to seismic. SRS can "fingerprint" such excitations in terms of their stress related time domain properties.

PPDF

A well known method used to characterize stress potent-ial of non-Gaussian excitations is rainflow analysis [8]. Rainflow analysis produces a plot known as a peak probability distribution function (PPDF). The PPDF differs from the instantaneous amplitude PDF in that it measures peaks only and not the instantaneous history of acceleration. There are

various forms of rainflow analysis. In general the resulting PPDF is a plot of the number of occurrences, n, of peaks having amplitudes within narrow ranges. In the case of vibration, PPDF counts the number of acceleration peaks with σ amplitudes that fall within defined range bins.

Standard practice for PPDF's for stress analysis is to plot them as single sided distributions. All peaks are summed together as in a first quadrant plot. Since stress is always positive, this makes sense.

The rainflow method used herein plots the number of bipolar peaks of acceleration as a two sided distribution. Knowing the mean value of the bipolar excitation peaks can be of importance in adjusting RS machine operation, and understanding the results of other analysis techniques.

There is a relationship between measured RMS level and the PPDF plot. One sigma on the plot is equivalent to the standard deviation of the PDF plot, which is equal to the RMS value of the excitation, assuming zero mean.

There are numerous rainflow and PPDF algorithms and their use has been recommended as a procedure in the SAE Fatigue Design handbook [9]. The special algorithm we use is based on the work of Dowling [10].

Plots produced by our rainflow algorithm, when applied to a narrow-band Gaussian random signal, may have a notch at the 0σ center. This is due to the fact that the number of cycles counted with a near zero magnitude is, of course, less than the number of cycles counted with a magnitude near or more than the RMS value.

AFDF

The PPDF is very useful in implementing various forms of Miner's rule of linear fatigue accumulation. The well known Miner's rule [11] states that an S-N curve can be used to compute total fatigue accumulation. We have adopted a form of Miner's rule using idealized S-N curves, below, as suggested by Crandall and Mark [12]:

$$AF = n\sigma^b$$

The terms of the equation are AF = Accumulated Fatigue, n = number of σ stress events, σ = the magnitude of the stress event, and b = the negative slope of a materials' log-log S-N curve.

From the above equation, it can be seen that sigma raised to the power function b (typically between 6 and 25 for the range of materials) has more of an effect on AF than the linear number of events per unit time. For the purposes of this paper, the value for copper, 10, was selected as being a typical value when using the above equation. The value as specified in MIL-STD-810E is 8. (For random ASD's, M=4=b/2.) Since it may be desirable to use more exact values of b than 10 or 8, our code has the ability to use any value entered by the user.

S-N data is taken using sine loading. In order to take into account the random nature of complex excitations, we sum the PPDF by accumulating fatigue for each σ interval from the above equation. This will accommodate the range of amplitudes of a chaotic signal, and make an estimate *proportional* to the total accumulated fatigue. The result is not exact for a complex device under test as it will be made up of various materials with different b values. The resultant sum is normalized for time in order to give a relative rate of fatigue accumulation.

$$AFDF = \sum_{\sigma=1}^{\sigma=x} (n_1\sigma_1^b + \ldots + n_x\sigma_x^b)$$

The terms for this equation are the same as for the first equation. The counts of n, produced by the rainflow analysis may be accumulated over any period of time.

It is important to point out that non-Gaussian excitation produced by a machine may not be the direct source of fatigue accumulation in a product. In cases where a component is free to vibrate at its own resonant frequency, it acts like a filter to the input excitation. Its response will be Gaussian regardless of excitation Gaussianity [13]. In effect, if two vibration machines producing equal excitation intensity, one Gaussian and the other non-Gaussian, are independently coupled to a linear system, the response of the system will be Gaussian and the accumulation of fatigue will be equal over the same time periods of excitation. In reality not all RS machines are capable of producing the same spectrum or intensity. Hence, they will have different capabilities to cause fatigue damage.

A general assumption from the above is that if one machine is producing higher levels of excitation than the other, the one with the higher power will produce a proportionately higher response in the linear system and hence, produce higher σ stress magnitudes, even though the PPDF's have otherwise equal distributions. As far as fatigue accumulation is concerned for a product under test, the controlling

variables will be excitation intensity, bandwidth, fixturing, and product character-istics.

Once AFDF's are estimated for the machine table, then effects of table loading, product and fixture transmissibility, table response vs temperature, or fixturing may be more accurately estimated than with ASD. AFDF measurements taken directly on a unit under test serve as the basis of comparison between tests, machines, fixtures, etc. AFDF may also be used to determine which type of shaker or table orientation produces the most rapid fatigue accumulation.

AFDF's can be calculated for both full range of σ and for $>2\sigma$ from the PPDF data. The reason for this is that all fatigue occurs at levels of stress greater than the materials fatigue limit, and 2σ is considered to near this limit. Software also allows the user to select a value of the power function b for the calculation.

Having taking many PPDF's on both RS and ED machines, we have found that RS machines produce greater numbers of stress event counts per unit time. This is probably related to the broader high frequency spectrum of RS machines and the fact that over short periods of time, their excitation is more transient in nature than random as produced by ED shakers. Even when producing the same magnitude of stress peak amplitudes, RS machines are more effective in accelerating fatigue rapidly because of the larger number of stress loadings per unit time. But since the stress peaks are also higher, the combination of both n and σ produces fatigue accumulation rates that range from tens to thousands of times higher for RS machines than for traditional shakers.

IV. MEASUREMENT OF ED MACHINES

It will be informative to see the comparative results from vibration measurements on both ED and RS machines.

After digitizing acceleration time history records from various ED shakers, analysis routines were applied by post processing the saved files.

The ASD shown in **Figure 1** is the result of ensemble averaging 127 windowed and 50% overlapped FFT's. All ASD's shown were processed identically. This particular data record used for this figure was 13 seconds in length and was comprised of 64K 12 bit samples. The shaker controller was set to produce a tailored ASD from 20Hz to 2000Hz at a level of 7gRMS. The signal recorded was table response.

Figure 1 shows the average spectral power density per unit bandwidth. Although the ASD proved that the excitation specification was successfully met, (which was the sole object of the test), the ASD and RMS values did not describe the higher stress producing peak levels produced by the excitation, unless we assume the data is Gaussian. An assessment of the fatigue accumulation using ASD is not direct and requires some additional calculation.

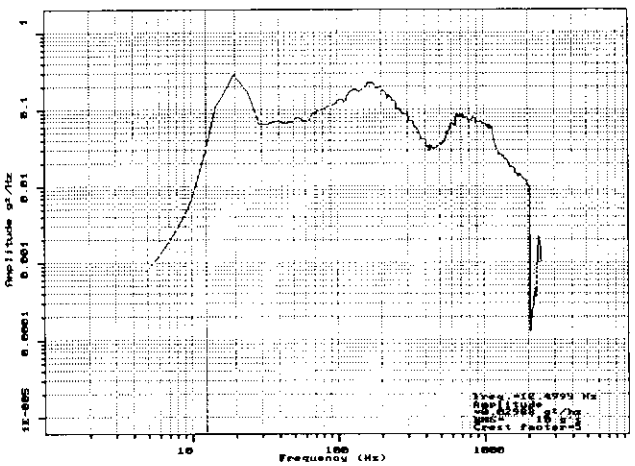

Figure 1. ASD produced by Gaussian random shaker.

Figure 2 shows the PPDF and AFDF of the ED shaker. It shows that the excitation is essentially random in nature and 3σ limited. The previously discussed notching of Gaussian PPDF's can be seen in this figure. While producing 6.9gRMS within the bandwidth of the ASD estimate, the highest number of stress events is less than 50/sec. The resulting AFDF's are; Full σ range = 4.30 E14, $>2\sigma$ = 2.22 E5.

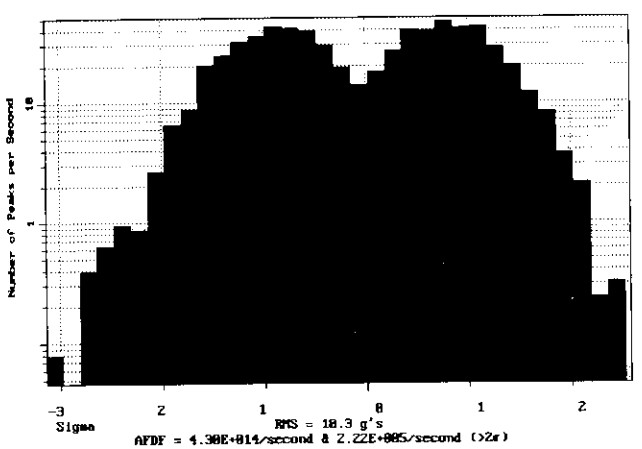

Figure 2. PPDF/AFDF of Figure 1 data, ED Gaussian random shaker.

Figure 3 is the SRS of the excitation calculated over the frequency interval of 1Hz to 2000Hz. SRS variables were 1/6th octave, damping = .05 of critical. The data record

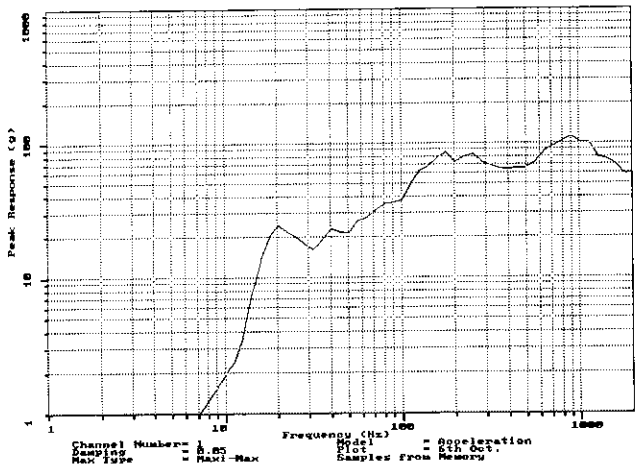

Figure 3. SRS from data used in Figure 1, Gaussian random shaker.

length processed was 13 seconds. The SRS shape is suggestive of the previous ASD in that the peaks of the SRS are at the same frequencies as the higher average spectral power maxima of the ASD. Although this plot represents only the peak response of a series of hypothetical oscillators to the excitation, it nevertheless gives us an indication of the potential of stress for linear response systems, plus a good deal about the spectral peaks of the excitation.

V. MEASUREMENTS ON RS MACHINES

To better understand the excitation produced by RS machines, it may be helpful to take a closer look at acceleration time data from one of these machines. The following data are from a multi-hammer RS machine with a solid table. Tests were recorded when running with only two of nine hammers, and then with all hammers in operation.

Figure 4, from a two hammer test, shows an expanded 0.05 sec portion of a 12.6 sec duration time record. Several damped sine waveforms from single impacts can be seen. The highest peak in this record is 48g's. The structure of the waveform is due to slight phase differences between individual hammers. When many hammers are in operation on a mode-rich table, the spectrum is more continuous and becomes more random-like. Also, there is a high probability that coincidence of individual wavefronts will result in both gain and attenuation due to constructive-destructive interference.

In **Figure 5,** all hammers of the same machine were in operation. The time record was 6.4sec. The waveform appears to be nearly stationary and random in nature. Peaks of various amplitudes can be seen, including one that is 72g with an overall level is 10gRMS. The existence of such peaks indicates a non-Gaussian PPDF with extended tails.

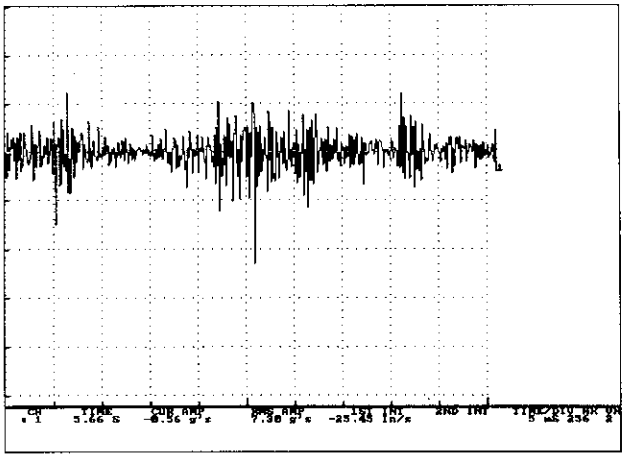

Figure 4. 0.05 sec time history of RS machine using only 2 hammers.

The ASD plot in **Figure 6** is from data in Figure 5. Of immediate significance is the general shape - an upslope at higher frequencies that extends to 5KHz. The primary significance of this plot is that there is more power at higher rather than lower frequencies, just the opposite of traditional shakers. This plot illustrates why most RS machines are very effective in screening small objects, such as electronic components which are most responsive to high frequencies. The spectral power reaches a maximum of $0.04g^2/Hz$ at 1454Hz. The overall 9.6gRMS is a typical average power. This particular machine was not being driven to maximum during this test, and was not loaded with products.

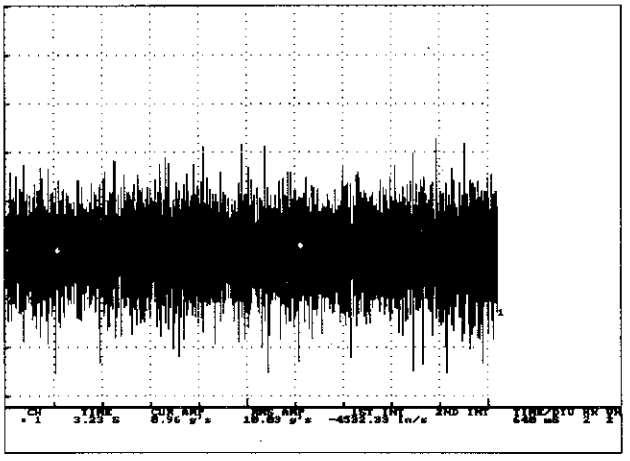

Figure 5. 6.4 sec time history from RS machine using 9 hammers.

In Figure 6 the peak at 30Hz is the line spectra associated with the hammer repetition rate. Hammer line spectra

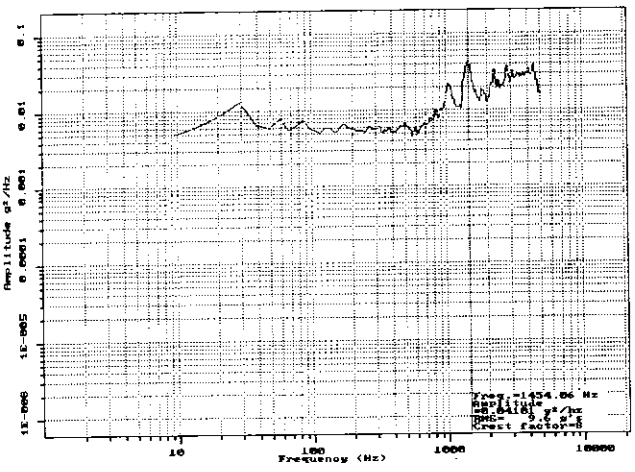

Figure 6. ASD from data used in Figure 5.

excites the gross translation modes of the table. Low frequency excitation, perhaps below 100Hz is useful for larger mass components, but has little effect on accumulated fatigue for small electronic components which resonate at much higher frequencies. In addition to the primary harmonic of the hammer repetition rate, higher order harmonics of 60Hz, 85-95Hz and higher, may also be seen. Table resonance peaks and impact waveform frequencies between 1KHz and 2Hz are obvious.

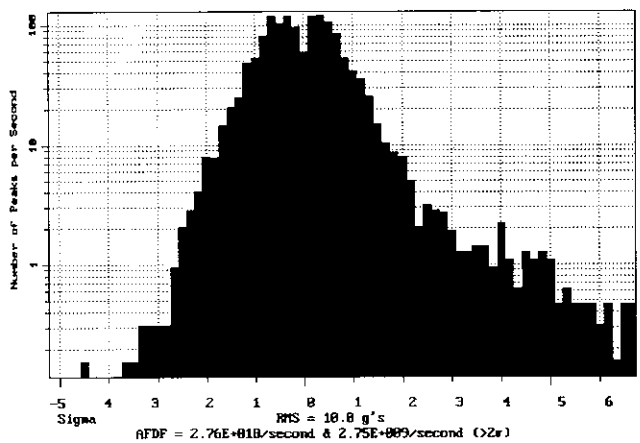

Figure 7. PPDF/AFDF from data used in Figure 5.

The PPDF plot with AFDF shown in **Figure 7** is from the 6.4sec record from the solid table machine data shown in figure 5. The RMS value is 10g's. The distribution exceeds 3σ indicating non-Gaussianity. The number of low sigma stress events approaches 120/sec. AFDF's are: all σ's = 2.76 E18, >2σ = 2.75 E9.

A comparison of PPDF and AFDF values for various RS and ED machines is given in **Table I.**

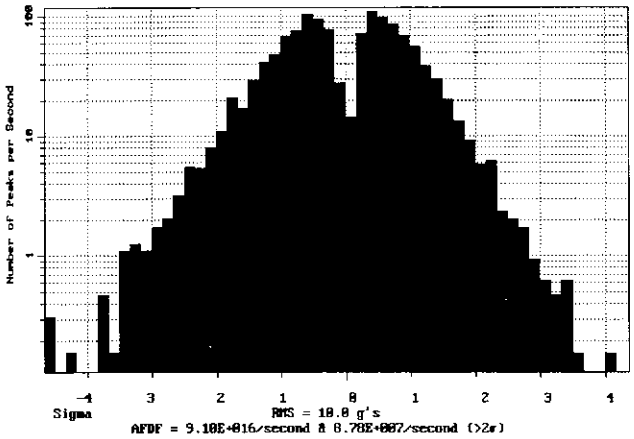

Figure 8. PPDF/AFDF from loaded solid table RS machine.

Figure 8 is a PPDF from a loaded, solid table machine. The PPDF and AFDF's are different than those from a similar RS machine in the previous figure. The distribution for this machine is close to a Gaussian PPDF, probably due to the table product interaction. The RMS level is 10.0g's, the number of events per second is 120, and the AFDF's are: all σ's = 9.10 E16, >2σ = 8.78 E7.

Our experience indicates that the highest AFDF numbers occur when fewer hammers are in operation on a solid table, or from a zone of a segmented table that is driven by only one or two hammers.

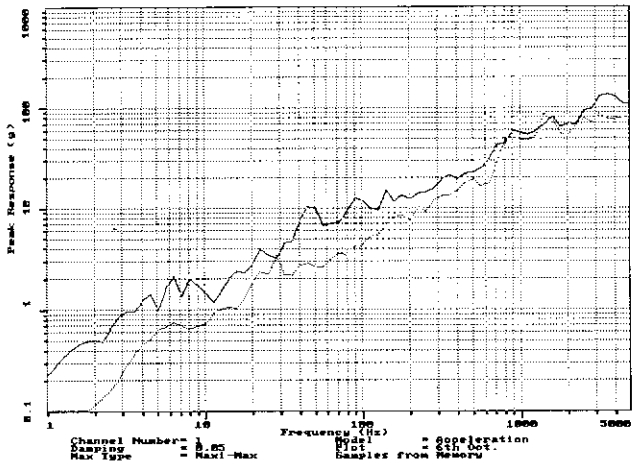

Figure 9. SRS plots of excitations from Figures 4 and 5.

Table 1. Comparative Fatigue Rate Values, Various Machines
All Machines were Normalized to 10gRMS

ED Machine	Peaks/Sec Max	All σ AFDF	>2σ AFDF	Note
a	50	5 E10	3.4 E4	Unloaded.
b.	45	3 E09	2.5 E3	Loaded.
Averages	47.5	2.65 E10	1.85 E4	
RS machines				
a.	240	3.11 E16	3.015 E7	Solid table under load.
b.	180	4.04 E16	4.80 E7	Solid, 2 Hammers
c.	95	7.54 E15	7.10 E6	Solid, All Hammers
c.	95	8.96 E16	8.78 E7	Solid, 2 Hammers
d.	120	2.74 E18	2.75 E9	Segmented, All
e.	170	3.05 E18	3.05 E9	Segmented, All
Averages	141.6	9.93 E17	9.95 E8	Averages and Ratios are valid only for the machines tested.
Ratio RS/ED	2.96:1	3.75 E7:1	5.41 E4:1	

The above phenomena has not been fully explored as of yet, but it is possibly due to a change in the excitation from an ongoing dynamic load type to a more transient load type. The transient load excitation would be comprised of high single peaks, similar to those seen in Figure 4.

Figure 9 is a dual SRS plot from the solid table RS machine running with 2 and 9 hammers. The solid line is the all hammer SRS, while the dotted line is the 2 hammer SRS. In this illustration, we can see a decrease in response spectrum magnitude at low frequencies with fewer hammers. This may further illustrate the result in the change in load spectrum discussed above.

The hammer repetition frequencies show up in both traces between 35 and 45Hz. The frequency shift is probably due to effects of air pressure change between the two tests, since no pressure adjustment on the supply manifold was made.

Differences in AFDF magnitude for various machines and combination of number of hammers/table design can be seen in Table I. In particular, the AFDF's computed for σ >2, the range where most fatigue will be accumulated, result in average differences of 10's of thousands when at the same RMS value. This should not mislead the user, however, because as in the case of Gaussian response of a simple resonator, the extended σ peaks from the table may not be too significant. The spectral power within the bandwidth of the response will be the controlling factor.

From Figure 9, one sees an indication that the modal response of the table is different depending on the number of hammers in operation. This is shown by differences in the two SRS traces at lower frequencies. It would appear that for this table, when excited by all hammers, there are response peaks at less than 10Hz.

VI. RELATED ANALYSIS ON RS MACHINES

While the forgoing has been focused on understanding and quantifying the excitation produced by RS machines, there are other applications of PPDF and AFDF that have more to do with evaluating product response. These applications are:

- Determination of screen intensity loss due to attenuation within a product. This reduces screen intensity on internal components of a complex product. In effect, such losses result in non-screening at the component level. A comparative measure of AFDF at the mounting point and

on the component of the product can give an estimate of screen intensity loss. If one is satisfied with average values, then an ensemble averaged transmissibility with coherence may be used.

- Determination of fixturing losses or gains. These can have the same effect as above, just as they do with traditional shakers. The same measurement techniques apply.

- Mapping an RS machine table. There are variations in performance across the surface of an RS machine table. Spectral power can be greatly altered by table loading, product feedback, temperature changes, etc. Again, the use of the suggested analysis techniques can identify these changes, by monitoring performance over time.

As an illustration of the above, the following data examples are from a product subjected to RS machine stresses.

VII. DATA FROM PATIENT MONITOR.

The following illustrations show relationships between excitation input and responses, using ASD, RMS, PPDF, and AFDF methods.

In this test, a hospital bedside patient monitoring and fluid supply device was screened using highly accelerated life testing procedures, known as HALT [14], while in the prototype stage. Sensors were located at the table product interface, as well as on a circuit card and fluid pump within the product. Orientation for all sensors was vertical.

Of importance were the findings of nearly Gaussian response of the internal circuit card and fluid pump, as well as the loaded table. Significant attenuation due to fixturing and product attenuation are also seen.

A summary of the PPDF and AFDF values are shown in **Table II.**

Zoomed-in 0.64sec time duration histories of excitation and response shown in **Figure 10** indicate a large reduction in excitation RMS amplitude between the machine table and the components inside the product. The reduction is 11.22gRMS to 1.38gRMS for the pump and to 3.15gRMS for the circuit card. The relationship between these changes is made more clear when apply-ing the tools we have discussed.

The ASD's show a loss in average spectral power for the table and components. The PPDF/AFDF's indicate reduced fatigue accumulation rates between the components and the table. And finally, the SRS's give the relationship between

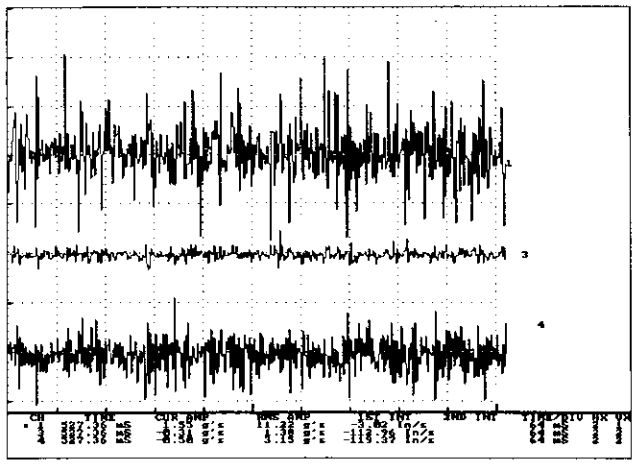

Figure 10. 0.64 sec time histories, Ch1=table, Ch3=fluid pump, Ch4=circuit card.

resonant peaks versus frequency, and in a rough but not perfect way, an idea about peak stress transmissibilities.

The loaded table ASD in **Figure 11** shows a marked decrease in spectral power at lower frequencies, probably due to table loading. Several of the spectral lines in this plot are probably due to the table/product combination. The overall intensity is 10gRMS and the spectrum has been attenuated about 1.5 orders of magnitude at frequencies less than 2KHz from the unloaded condition of this particular RS machine.

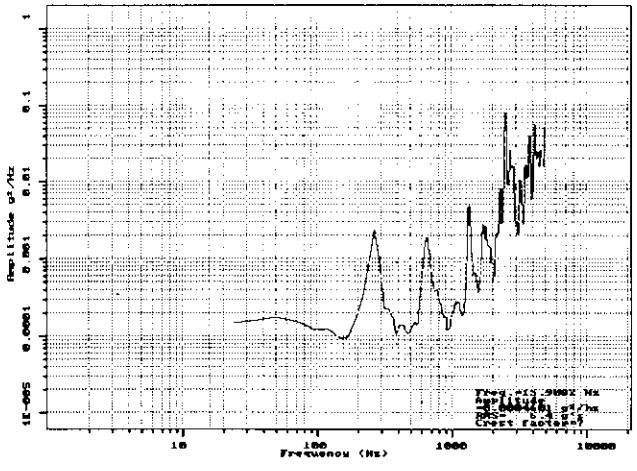

Figure 11. ASD of table data from Figure 10.

Figure 12 is from the table and shows a near-Gaussian PPDF with tails out to 3σ, stress events at over 240/second, and an intensity level of 10.0gRMS. The AFDF's are: All σ = 3.07 E16, and $>2\sigma$ = 2.92 E7. The high loading rate

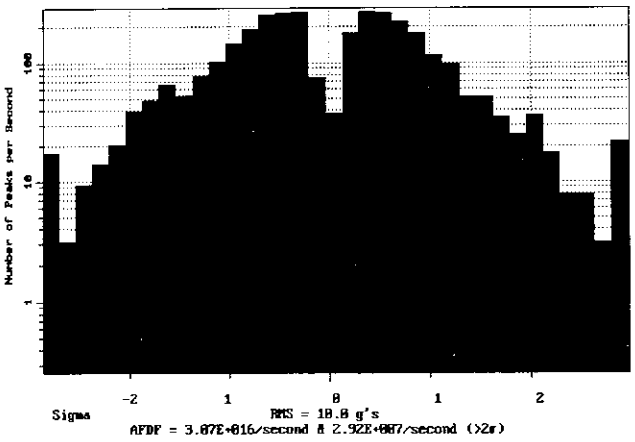

Figure 12. PPDF/AFDF from table data in Figure 10.

counts at the sigma extremes is due to the combination of the scaling and time normalization of the less than one second duration of the test record, in this case 0.064sec. In other words, if only 1 event of high sigma occurs during an analysis window that is shorter than one second, the number of events normalized to one second will have the distribution cutoff shape as seen in Figures 3, 13, and 15. In addition, the distribution may not be continuous.

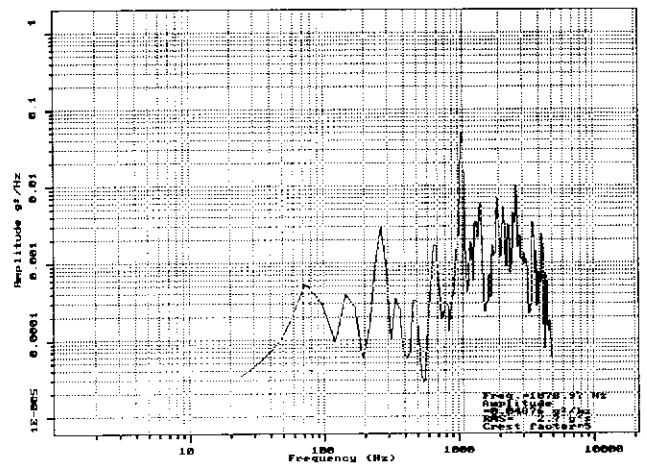

Figure 13. ASD of circuit card data in Figure 10.

Figure 13 shows the ASD of the printed circuit card. Except for the major 0.003 g^2/Hz peak at 280Hz, which correlates exactly with the peak seen in the table ASD, Figure 11, this component responds differently than the table. Since the circuit card resonance acts as a bandpass filter on the excitation, the response of the card would be expected to be Gaussian no matter what form of excitation is applied, as long as it is ongoing and random, per Papoulis [15].

The near perfect Gaussian PPDF from the circuit card in **Figure 14** is a prime example of the above. The degree of loss between the excitation and the Gaussian response of the card are shown by both the reduced RMS and AFDF values. Note that the RMS value is down to 3.2gRMS from 11.2gRMS, the number of peaks is still in the 200's/sec, and the AFDF's are down to: all σ = 1.21 E11, and $>2\sigma$ = 3.04 E6. These are very significant reductions. This illustrates the fact that complete products may be difficult to screen and it may be necessary to screen individual components of a product independently when using HALT.

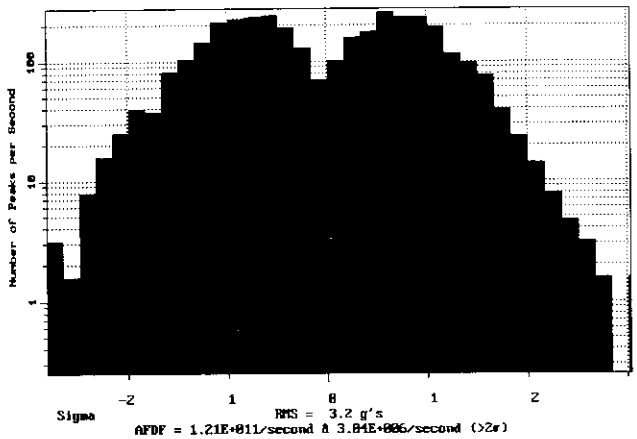

Figure 14. PPDF/AFDF from circuit card data in Figure 10.

For large mass objects, direct excitation is the only efficient way to couple in high stress excitation. The same analytical techniques as described for machines also apply to direct excitation.

The above may not be strictly true for reduced intensity screens as used for production sampling.

Looking at the fluid pump, the ASD in **Figure 15** shows a similar reduction in average power, particularly at high frequencies above 1KHz. A new high peak is seen at about 60-70Hz, due do the primary resonance of the pump itself. It is likely that the pump is acting in the same self-resonance manner as the circuit card except that its resonance is lower.

The PPDF and AFDF of the pump in **Figure 16** echo the results of the circuit card case. AFDF's are down to: all σ = 6.11 E5, $>2\sigma$ = 2.25 E4. The number of peaks is still high, over 200/sec, and the probability skirts terminate at 3σ for the near Gaussian PPDF.

Like the circuit card, maximum screen intensity is probably being lost due to losses through the product structure in a

Table II. Summary of AFDF readings during HALT.

	Counts/sec.	AFDF, all	AFDF >2σ	gRMS.
Table	240's	3.07 E16	2.92 E7	10.0
CB	230's	1.21 E11	3.04 E6	3.2
Pump	240's	6.11 E5	2.25 E4	1.4

manner similar to fixturing. This component would certainly be an excellent candidate for direct excitation outside of the product.

The reduction in excitation mentioned above from the table to the pump within the medical product is further confirmed by the estimate of classical transmissibility and coherence as seen in **Figure 17.** The coherence is highest at about 1200Hz but shows a complete lack of phase relationship below and above this frequency, an additional indication that the pump is resonating within its own spectrum.

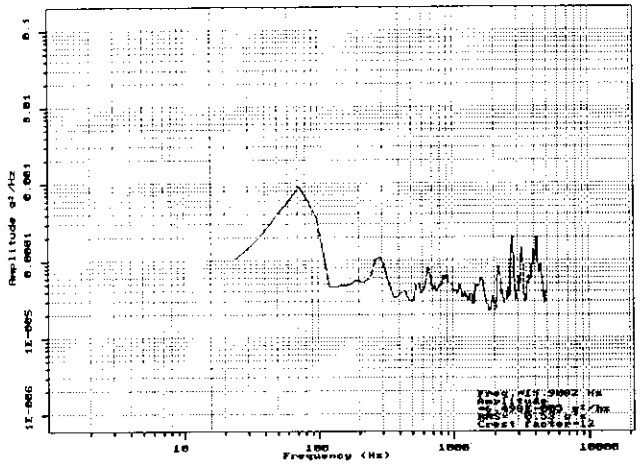

Figure 15. ASD of fluid pump data in Figure 10.

Figure 18 shows the combination SRS plots from the components monitored during the test. The table excitation is shown by the solid line, the pump by the fine dotted line, and the circuit card by the heavier dashed line. These plots give some idea as to peak product component response with regard to the table in terms of amplitude loss or gain with frequency.

It can be seen that the component SRS's are attenuated,

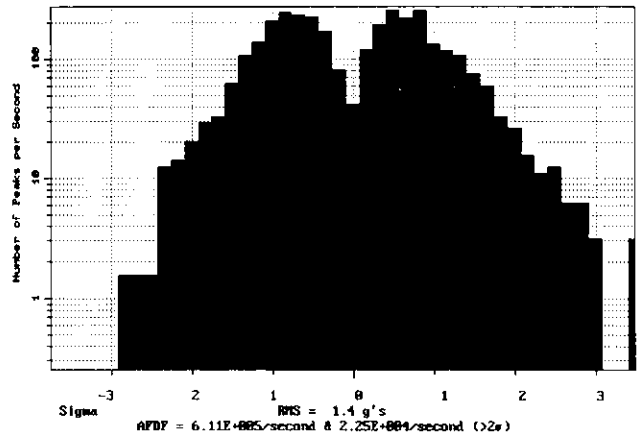

Figure 16. PPDF/AFDF from fluid pump data in Figure 10.

except some gain occurs for both the circuit card and the pump at 80Hz. There is additional gain for the circuit card near 1KHz, which corresponds to the major resonant point in the ASD in Figure 13. The reduction in high frequency amplitude between the table and circuit card and pump traces, reflects the reduced high frequencies present as shown by the ASD and transmissibility plots. Although it is commonly done, SRS is not a good measure of peak transmissibility. The problem is that time domain estimates contain no phase information.

VII. CROSS TABLE TRANSMISSIBILITY

Transmissibility can also be used to study cross table performance. Measurements made on a particular RS machine, with sensors 24 inches apart and sensitive axis in the plane of the table resulted in the following findings: 1) There was a difference of about 3:1 in average spectral power between the two locations, 2) there was a single frequency for which phase coherence was greater than 50% (3KHz), and 3) aside from this single frequency, there was

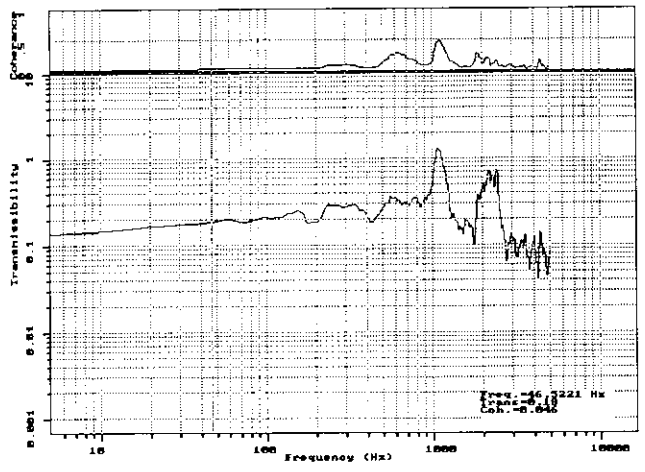

Figure 17. Transmissibility/Coherence between table and fluid pump data in Figure 10.

almost zero coherence at all other frequencies. This indicates the existence of acceleration vectors which have magnitude but no phase relationship, i.e., rotational couples.

The spectral average power difference of 3:1 in between two table locations is not uncommon for RS machines. Proximity of the sensor position to a hammer, hammer performance, table damping and modes, and thermal gradients, etc., will dictate the magnitude of differences.

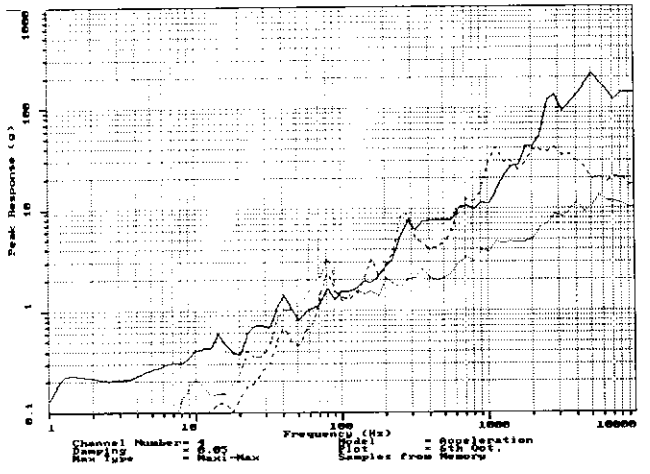

Figure 18. SRS plots of table (solid), fluid pump (dotted), and circuit card (dashed) from data in Figure 10.

Finally, just a mention of the relevance of measuring acceleration and making a jump to stress. When a component of a spring mass system is subjected to acceleration, its motion will result in stress within the supporting structure. The stress produced is pro-portional to the acceleration of the spring mass system, and this stress results in fatigue accumulation. See again Crandall [16].

X. CONCLUSIONS

1. The RS machine is not a true stationary Gaussian random shaker. It is better characterized as a high repetition rate shock machine producing ongoing dynamic, random-like loading. An investigation of short term time history waveforms confirms this.

2. The success of RS machines for CSS is primarily due to their ability to greatly shorten the time for defect precipitation. This is because of three characteristics: a) Very high intensity, b) Broad spectral band, and c) Simultaneous multi-axis and rotational excitation. In some cases, the non-Gaussian excitation is made Gaussian by the resonance filtering of the item under stress. However, the magnitude of the response can be driven to very high levels at high loading rates, resulting in high fatigue accumulation rates.

3. Characterization of the fatigue inducing potential of RS machines is more accurately done with rainflow PPDF rather than ASD and RMS methods, neither of which account for the number of stress loadings per unit time nor the peak amplitude domain of either Gaussian or non-Gaussian vibration.

4. An AFDF "figure of merit" for both Gaussian and non-Gaussian source/response assessment, as described in this paper, can give a useful measure of relative fatigue accumulation rate. This tool is applicable to machine performance, product response and stress transmissibility. The AFDF can also be used for characterizing field excitations in terms of their fatigue producing potentials.

AFDF does not produce an absolute value of fatigue accumulation for all components of an item under test. That would require a change in S/N slope b for each material involved. Rather the intent is to compare excitations and responses, in order to find their relative stress producing rates. A similar figure of merit function has been proposed by Kececloglu and Li [17] which applies to general damage.

ACKNOWLEDGEMENTS

The author is indebted to the invaluable technical advice and research provided by Allan Piersol, and to the support of others in the industry who have encouraged the author to develop methods to characterize RS machines.

References

1. Ashmore, S.C., Piersol, A.G., Witte, J.J., "Accelerated Service Life Testing of Automotive Vehicles on a Test Course," *Vehicle System Dynamics,* Vol.21., pp. 89-108. 1992.

2. Szymkowiak, E.A., "Vibration Mechanics in Environmental Stress Screening", Presented at IES ESSEH Workshop, Baltimore, MD., Oct. 1992. (Copies may be obtained from this author)

3. Henderson, G.R., "RS6DOF Screening Machines, How They Work - How to Evaluate Them", Presented at IES ESSEH Workshop, Baltimore, MD., Oct. 1992.

4. Scharton, T.D., "Development of Impedance Simulation Fixtures for Spacecraft Vibration Tests", NASA CR-1352, Langley Research Center, VA, May 1969.

5. Scharton, T.D., "Analysis of Dual Control Vibration Testing", *Proceedings, Institute of Environmental Sciences*, pp. 140-146, New Orleans, LA, 1990.

6. Biot, M.A., "Theory of Elastic System Vibration Response under Transient Excitation with an Application to Earthquake Resistant Buildings", *Journal of Applied Sciences,* Vol. 19, pp. 260-268. 1933.

7. Smithson, S.A., "Shock Response Spectrum Analysis for ESS and STRIFE/HALT Measurements", *Proceedings, Institute of Environmental Sciences,* San Diego, CA. 1991.

8. Dowling, N.E., "Fatigue Failure Predictions for Complicated Stress-Strain Histories", *Journal of Materials,* Vol. 7, No. 1, pp V-1 to V-17, 1972.

9. Rice, R.C., *Fatigue Design Handbook,* 2nd Edition, Society of Automotive engineers, Warrendale, PA, 1988.

10. Dowling, ibid 8.

11. Miner, M.A., "Cumulative Damage in fatigue", *Journal of Applied Mechanics,* Vol. 12. p. 159, 1945.

12. Crandall, S.H., Mark, W.D., *Random Vibration in Mechanical Systems,* Academic Press, New Your, NY, 1963.

13. Papoulis, A., "Narrow-Band Systems and Gaussianity", RADC-TR-225, Rome Air Development Center, Griffis AFB, New York, NY., Nov. 1971.

14. Hobbs, G.K., "Highly Accelerated Life Tests - HALT", unpublished seminar notes, Hobbs Engineering, Westminister, CO., 1990.

15. ibid 13.

16. ibid, 12.

17. Kececloglu, D., and Li, Dingjun., "Accelerated Testing of Mechanical Equipment", Paper 861667, SAE Aerospace Technology Conference, Long Beach, CA. Oct. 1986.